Structural and magnetic phase transitions in shape-memory alloys $Ni_{2+x}Mn_{1-x}Ga$

A. N. Vasil'ev, A. D. Bozhko, and V. V. Khovailo
Moscow State University, Moscow 119899, Russia

I. E. Dikshtein and V. G. Shavrov
Institute of Radioengineering and Electronics of RAS, Moscow 103907, Russia

V. D. Buchelnikov
Chelyabinsk State University, Chelyabinsk 454021, Russia

M. Matsumoto
Institute of Advanced Material Processing, Tohoku University, Sendai 980-77, Japan

S. Suzuki, T. Takagi, and J. Tani
Institute of Fluid Science, Tohoku University, Sendai 980-77, Japan
(Received 7 May 1998)

The Heusler-type alloy $Ni_{2+x}Mn_{1-x}Ga$ exhibits well defined shape memory properties in a ferromagnetic state, which means that the martensitic transition temperature is lower than the Curie point of this material. The change of composition makes these characteristic temperatures approach each other. To study this behavior, the measurements of specific heat, ac magnetic susceptibility, and dc resistivity were performed. The phase diagram of the cubic ferromagnet describing possible structural and magnetic transitions is obtained theoretically. This diagram is compared with experimental data on $Ni_{2+x}Mn_{1-x}Ga$. An estimate is given of the magnetic-field influence on the temperature of martensitic transformation in the studied alloys. [S0163-1829(99)09701-5]

I. INTRODUCTION

Some representatives of the Heusler alloy family are known to exhibit a crystallographically reversible, thermoelastic martensitic transformation resulting in the shape-memory effect. In most cases the shape-memory alloys are *nonmagnetic* and the options to influence their shape and dimensions are restricted to stress and temperature. In Mn-containing Heusler alloys, however, the indirect exchange interaction between magnetic ions results in ferromagnetism. It opens the possibility to influence the shape and dimensions of *magnetic* shape-memory alloys by an external magnetic field in addition to stress and temperature. This new possibility can be realized through the magnetically driven shift of the structural transition temperature. The most promising means by which to achieve a substantial effect on shape and dimensions of ferromagnetic shape-memory alloys through the application of a magnetic field seems to be the merging of the temperatures of structural and magnetic transitions. In this case the application of a magnetic field would result in a martensitic transformation. To realize this effect it is initially necessary to determine the correct alloy composition. Subsequently, it is necessary to define the main physical parameters of this alloy and to estimate the influence of a magnetic field on the temperature of the structural phase transition.

A Mn-containing Heusler-type alloy, Ni_2MnGa, experiences martensitic transformation when in a ferromagnetic state. The temperatures of ferromagnetic ($T_C = 376$ K) and structural ($T_M = 202$ K) transitions differ significantly for the stoichiometric composition. Altering the composition allows a change of these characteristic temperatures.

In the present work the partial substitution of Mn with Ni increased T_M and decreased T_C, resulting in their coincidence. A complex study of the physical properties of $Ni_{2+x}Mn_{1-x}Ga$ alloys in the range of $x = 0-0.2$ was performed. The theoretical analysis of the possible structural and magnetic phase transitions in the cubic ferromagnet was given and the obtained results were compared with existing experimental data. The possibility of a first-order magnetic phase transition in $Ni_{2+x}Mn_{1-x}Ga$ is discussed and estimates of magnetic-field and pressure effects on the temperature of the structural phase transition are given.

The paper is organized in the following way. Section II contains information on the physical properties of stoichiometric and nonstoichiometric Ni_2MnGa and presents the main parameters of these compounds. The results of the experimental studies of resistivity, specific heat, and magnetic properties of $Ni_{2+x}Mn_{1-x}Ga$ alloys are presented in Sec. III. Section IV contains theoretical treatment of structural and magnetic phase transitions based on Landau's phenomenological approach. The effect of a magnetic field on the martensitic transition temperature is estimated by using a thermodynamic model. The experimental and theoretical results are compared in Sec. V.

II. FERROMAGNETIC SHAPE-MEMORY ALLOYS $Ni_{2+x}Mn_{1-x}Ga$

A. Stoichiometric composition

A detailed study of magnetic order and phase transformation in stoichiometric Ni_2MnGa was performed by Webster *et al.*[1] The intermetallic compound Ni_2MnGa is a ferromagnetic Heusler alloy with $L2_1$ structure. Ni ions occupy the corner sites of the body-centered-cubic structure, while Mn and Ga ions occupy alternate body-center sites. Structural phase transition from the cubic austenite ($a=0.582$ nm at $T=295$ K) to the tetragonal martensite ($a=0.592$ nm and $c=0.557$ nm at $T=4.2$ K) takes place on cooling below $T_M=202$ K. This phase transition is hysteretic, but reversible on heating, showing the shape-memory effect. The measurements of magnetization M of Ni_2MnGa revealed behavior typical of a soft ferromagnet above T_M. Below this temperature, however, an abrupt decrease of M was observed, indicating an increase of the magnetic anisotropy and a reduction in the number of easy axes of magnetization. Magnetization saturates to a value of $M\approx 80$ kA/m in the field $H\geqslant 1200$ kA/m. Neutron-diffraction measurements showed that magnetic moments of about $4\mu_B$ are oriented along the [111] direction in austenitic phase and are mainly confined to the Mn sites. In contrast, Ni ions possess moments of less then $0.3\mu_B$. The Curie temperature for the stoichiometric composition of Ni_2MnGa is $T_C=376$ K. The temperatures of ferromagnetic and martensitic transitions were found to be quite sensitive to distances between Mn ions. The application of hydrostatic pressure to stoichiometric Ni_2MnGa resulted in the increase of the ferromagnetic transition temperature $dT_C/dP=2.8$ K/kbar and in the decrease of the martensitic transition temperature $dT_M/dP=-1.5$ K/kbar (Ref. 2).

B. Nonstoichiometric composition

Judging by phase-transition temperatures most samples of Ni_2MnGa used in numerous recent studies were of nonstoichiometric compositions. Martensitic transition temperature T_M ranging between 160 K and 450 K have been reported (Refs. 3–13). The main feature of these studies was observation of various premartensitic and intermartensitic transformations accompanied by the appearance of long-range modulations of the crystal lattice.

A modulated structure constituted by a shifting of (110) planes along the $[1\bar{1}0]$ direction with a periodicity of five atomic layers has been observed in a martensite produced by cooling through transition.[3] Moreover, further structural transformations were induced by an external stress in the martensitic phase.[4] The measurements of diffuse x-ray intensity from a single crystal of Ni_2MnGa with $T_M=160-180$ K have revealed a strong soft-mode behavior in the transverse acoustic phonon branch, with q in the [110] direction and polarization in the $[1\bar{1}0]$ direction in the high-temperature phase.[5] Condensation of this phonon mode resulted in the formation of the premartensitic phase in the temperature range $T_M<T<T_1=220$ K (Refs. 6 and 7). The soft mode was also found in inelastic neutron-scattering measurements of single crystals of Ni_2MnGa with $T_M=220$ K (Refs. 8 and 9) and $T_M=284$ K (Ref. 10). Significant, though incomplete softening in the $[\zeta,\zeta,0]TA_2$ phonon branch has been observed at a wave vector $\zeta_0\approx 0.33$. The anomaly in the dispersion curve was shown to persist at high temperatures, even above the Curie point. A temperature-dependent peak in the elastic diffuse scattering was also present at the wave vector ζ_0, which developed into a Bragg peak, representative of an intermediate phase between the high-temperature Heusler and the low-temperature martensitic structures. The intermediate phase transition at $T_1=265$ K in the sample with $T_M=220$ K was confirmed by ultrasonic studies.[11,12] Significant softening of elastic constants was found when approaching this temperature. The behavior of velocity and attenuation in this premartensitic phase was found to be consistent with neutron-scattering data and showed that the premartensitic phase is an ordered modulated phase. In a recent paper[13] the martensitic transformation sequence in two single crystals of Ni-Mn-Ga alloys with a martensite start temperature of about 400 K was investigated using multiple experimental techniques. A two-step thermally induced martensitic transformation during cooling and one-step reverse transformation during heating was found in both alloys, although different modulated martensitic phases existed in each of the alloys.

In comparison to the study of structural transformations, the changes of magnetic properties and the ferromagnetic transition in Ni_2MnGa itself was less thoroughly investigated. In both stoichiometric and nonstoichiometric alloys, the transition into martensitic phase is accompanied by a decrease of low-field magnetic susceptibility and by a 10–20% increase in the magnetization of saturation M_S (Refs. 14–16). The influence of nonstoichiometry (Ni excess) on the structural and magnetic properties of $Ni_{2+x}Mn_{1-x}Ga$ was studied in Ref. 17. While almost no shift of the Curie temperature was evidenced at $x=0.1$, no martensitic phase transition was found for this alloy up to T_C.

In order to clarify this extremely unclear situation concerning the composition dependencies of martensitic and magnetic transition temperatures, we undertook a complex study of various physical properties of $Ni_{2+x}Mn_{1-x}Ga$ in the range of $x=0-0.20$. Changing the composition results in the variation of the conduction electrons density. The importance of the conduction electrons in stabilizing the Heusler structure was noted by Hume-Rothery[18] a long time ago. It was suggested[19] that the structure is stabilized because the Fermi surface barely touches the (110) Brillouin-zone boundary. Comparing the density of states of cubic and tetragonal structures in Ni_2MnGa (Ref. 20), it was suggested that the band Jahn-Teller effect causes the lattice transformation in this alloy. Since the exchange interaction involves the polarization of conduction electrons, any change of the chemical order may directly influence the alloy's magnetic behavior. In order to increase the martensitic transition temperature T_M and to decrease the ferromagnetic transition temperature T_C we undertook a partial substitution of Mn sites with Ni ions. This resulted in an increase of the electron population as well as in negative chemical pressure.

III. EXPERIMENTAL RESULTS

A. Samples

The ingots of $Ni_{2+x}Mn_{1-x}Ga$ samples of various compositions were prepared by arc melting high-purity (99.99%)

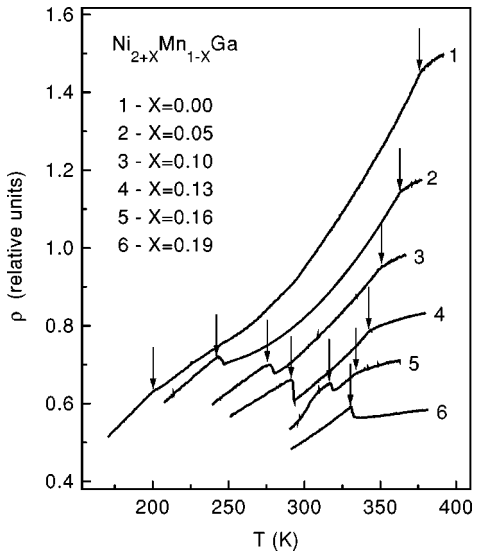

FIG. 1. Temperature dependencies of dc resistivity in $Ni_{2+x}Mn_{1-x}Ga$ ($x=0-0.20$).

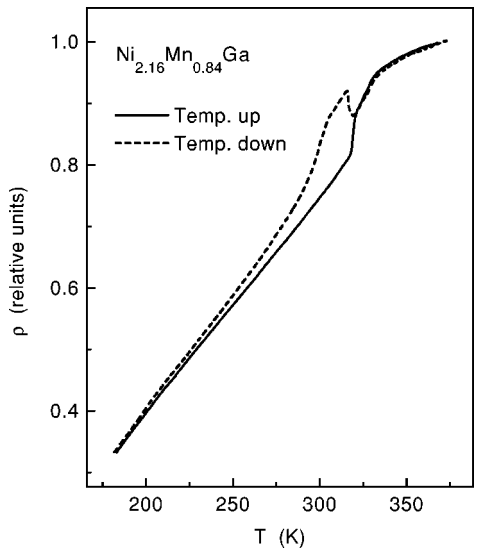

FIG. 2. Temperature dependencies of dc resistivity in $Ni_{2.16}Mn_{0.84}Ga$.

elements and subsequent homogenization of the ingot material by annealing at 1100 K for 9 days. The ingots were quenched in ice water. While quenching is considered to be important to obtain the highest degree of chemical order it also increases the brittleness of the samples. The composition of the samples was characterized by Ni excess x in the range $x=0-0.20$. The crystal structure of the samples at room temperature was determined by x-ray diffraction using Cu K_α radiation. In order to measure electrical resistivity, specific heat, and magnetic properties, samples of various shapes were spark cut from the homogenized ingots.

B. Electrical resistivity

Direct current resistivity measurements provide a simple and effective tool to detect both structural and magnetic transitions. As shown in Fig. 1, at T_M the resistivity exhibits a pronounced jumplike behavior, while at T_C only change in the slope takes place. The steepening of slopes in the ferromagnetic phase can be attributed to the disappearance of electrons scattering on magnetic fluctuations. Resistivity measurements allow distinction of the martensitic and magnetic transitions, even if their temperatures are in close proximity. As Ni content increases, T_M gradually increases and T_C gradually decreases until these temperatures merge in the samples with $x\geqslant 0.18$. In these samples the jump of resistivity is directly followed by a steepening of the slope. No hysteresis was observed at ferromagnetic transition, while below the martensitic transition the resistivity showed a marked hysteretic behavior. Surprisingly, in the samples with high Ni content the hysteresis, as shown in Fig. 2, becomes extremely wide, extending up to several tens of degrees.

C. Differential scanning calorimetry

The hidden heat of transformations was measured using the differential scanning calorimetry (DSC) technique. The martensitic transformation was accompanied by well-defined peaks in the specific heat due to the hidden heat of transition, which is a characteristic of first-order phase transitions. The second-order ferromagnetic phase transitions were accompanied by jumps in the specific heat. The character of anomalies changed significantly (from jumps to peaks) in the samples where the temperatures of the structural and magnetic phase transitions merged. This indicates that the ferromagnetic phase transitions in these samples became first-order transitions. Both martensitic and ferromagnetic phase transitions were accompanied by exothermic and endothermic peaks at cooling and heating, respectively. The dependencies observed in the samples of six different compositions at cooling are shown in Fig. 3. Due to the relatively large width of the peaks the DSC technique does not allow distinction between the two transitions when they are close in temperature. These measurements show, however, that T_M

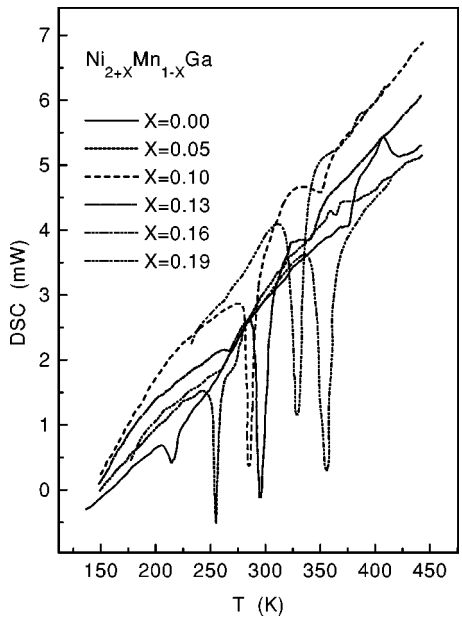

FIG. 3. Differential scanning calorimetry scans of $Ni_{2+x}Mn_{1-x}Ga$ at heating.

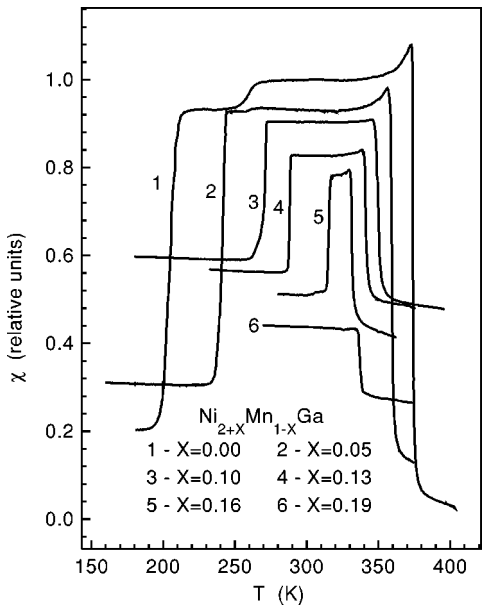

FIG. 4. Temperature dependencies of low-field magnetic susceptibility of $Ni_{2+x}Mn_{1-x}Ga$.

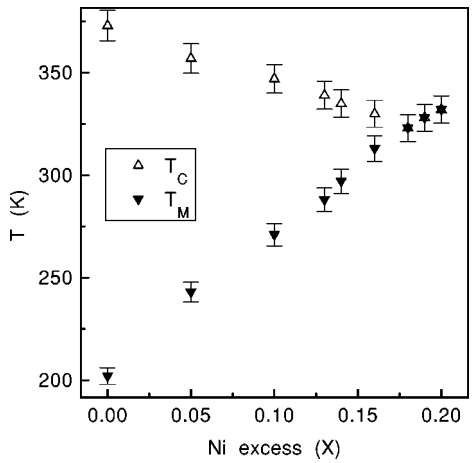

FIG. 5. The composition dependencies of the ferromagnetic transition temperature T_C and the martensitic transition temperature T_M in $Ni_{2+x}Mn_{1-x}Ga$ ($x=0-0.20$).

and T_C merge at composition $x \geqslant 0.18$ and that the temperature of the mixed transition increases. The estimate of the hidden heat of martensitic transition in $Ni_{2.19}Mn_{0.81}Ga$ is $Q = 4\times10^7$ J/m^3.

D. Magnetic measurements

The temperature dependencies of the low-field ac magnetic susceptibility χ, as shown in Fig. 4, exhibit very sharp changes at martensitic and magnetic transitions. The martensitic phase transition from the cubic to the tetragonal structure is indicated by the drastic drop of χ. χ also sharply decreases at the Curie temperature when the ferromagnetic phase is destroyed. While T_M and T_C are still separated in $Ni_{2.16}Mn_{0.84}Ga$ and two anomalies occur, in $Ni_{2.19}Mn_{0.81}Ga$ only one anomaly of ac magnetic susceptibility at the mixed phase transition is observed.

The general tendency of T_M to increase and of T_C to decrease with the change in composition before they merge is illustrated by Fig. 5, where the temperatures of phase transitions are presented as the averages of various measurements.

In the course of the present study we undertook an attempt to realize the austenite-martensite transformation under the influence of pulsed magnetic field up to 24 000 kA/m. To measure the spontaneous striction of this transition, a thin plate of quartz was glued to the surface of the sample. It was found that the magnetostrictive tension increases in λ-like manner when approaching T_M (Ref. 15), but every attempt to measure magnetostriction in close proximity to the martensitic transition temperature ended in the destruction of either the quartz transducer, or the sample itself.

IV. THERMODYNAMIC THEORY

The experimental results presented above show that the temperatures of magnetic and structural phase transitions approach each other and even merge due to the change of alloy composition. This behavior can be described within a phenomenological model based on Landau's expansion of free energy.

A. Phase diagram of cubic ferromagnet

Let us consider a cubic metal of space group O_h experiencing at cooling ferromagnetic and structural phase transitions. The order parameters responsible for the structure transformation are the combinations of the deformation tensor components e_{ik}. The magnetic phase transition is described by the components of magnetization **M**. The thermodynamic potential for such a system can be written as

$$\Phi = \frac{1}{2}(c_{11}+2c_{12})e_1^2 + \frac{1}{2}a(e_2^2+e_3^2) + \frac{1}{2}c_{44}(e_4^2+e_5^2+e_6^2) + \frac{1}{3}be_3(e_3^2-3e_2^2) + \frac{1}{4}c(e_2^2+e_3^2)^2 + \frac{1}{\sqrt{3}}B_1e_1m^2$$

$$+ B_2\left(\frac{1}{\sqrt{2}}e_2(m_1^2-m_2^2) + \frac{1}{\sqrt{6}}e_3(3m_3^2-m^2)\right) + B_3(e_4m_1m_2+e_5m_2m_3+e_6m_3m_1) + \frac{1}{2}\alpha_1(m_1^2+m_2^2+m_3^2)$$

$$+ \frac{1}{4}\delta_1(m_1^2+m_2^2+m_3^2)^2 + K_1(m_1^2m_2^2+m_2^2m_3^2+m_3^2m_1^2) - \nu Te_1. \quad (1)$$

Here e_i are the linear combinations of the deformation tensor components e_{ik}: $e_1=(e_{xx}+e_{yy}+e_{zz})/\sqrt{3}$, $e_2=(e_{xx}-e_{yy})/\sqrt{2}$, $e_3=(2e_{zz}-e_{xx}-e_{yy})$, $e_4=e_{xy}$, $e_5=e_{yz}$, $e_6=e_{zx}$, a, b, and c are the linear combinations of the second-, third-, and fourth-order elastic moduli, respectively, $a=c_{11}-c_{12}$, $b=(c_{111}-c_{112}+c_{123})/6\sqrt{6}$, $c=(c_{1111}+c_{1112}-3c_{1122}-8c_{1123})/48$, $\mathbf{m}=\mathbf{M}/M_S$, M_S is the saturation magnetization; α_1 and δ_1 are the exchange constants, B_1, B_2, and B_3 are the exchange magnetostriction and relativistic magnetostriction constants, K_1 is the first cubic anisotropy constant, ν is the coefficient of thermal expansion. The elastic modulus $a=c_{11}-c_{12}$ tends to zero, while approaching the structural phase transition temperature, and in the vicinity of phase transition it is described by the equation $a=a_0(T-T_M)$. The cubic symmetry of the crystal allows the consideration of the third-order term in formulas (1) that will result in the first-order structural phase transition.

The thermodynamic potential (1) describes both the case of T_M and T_C coincidence and the case of T_C and T_M separation. In the first case the magnetic moment changes in magnitude and direction at phase transition. In the second case (for $T_C>T_M$) the structural phase transition is accompanied mainly by a change in the magnetic moment direction.

The most interesting case, the close proximity of T_C and T_M, will be considered below. The minimization of the thermodynamic potential (1) with respect to the deformation tensor components e_1, e_4, e_5, and e_6 leads to the following equation:

$$\Phi=\Phi_0+\frac{1}{2}a(e_2^2+e_3^2)+\frac{1}{3}be_3(e_3^2-3e_2^2)+\frac{1}{4}c(e_2^2+e_3^2)^2+B_2\left(\frac{1}{\sqrt{2}}e_2(m_1^2-m_2^2)+\frac{1}{\sqrt{6}}e_3(3m_3^2-m^2)\right)+\frac{1}{2}\alpha(m_1^2+m_2^2+m_3^2)+\frac{1}{4}\delta(m_1^2+m_2^2+m_3^2)^2+K(m_1^2m_2^2+m_2^2m_3^2+m_3^2m_1^2), \quad (2)$$

where $\alpha=\alpha_1+\nu B_1T/[3^{1/2}(c_{11}+2c_{12})]$, $\delta=\delta_1-B_1^2/[6(c_{11}+2c_{12})]$, $K=K_1-B_3^2/2c_{44}$ are the exchange constants and the first cubic anisotropy constant renormalized by magnetostriction. We assume that the exchange-interaction parameter α decreases linearly when approaching the Curie point, i.e., $\alpha=\alpha_0(T-T_C)$.

The minimization of the thermodynamic potential (2) with respect to the rest of the variables e_2, e_3, m_1, m_2, and m_3 makes it possible to determine all feasible structural and magnetic phases. As a result the following phases of the ferromagnet and their stability conditions are found (in this consideration it is assumed that $b>0$, $K<0$, and $B_2=B$).

(1) The cubic paramagnetic phase,

$$m_1=m_2=m_3=0,\ e_2=e_3=0,$$

is stable at $\alpha\geqslant 0$, $a\geqslant 0$.

(2) The tetragonal paramagnetic phase,

$$m_1=m_2=m_3=0,\ e_2=0,\ e_3=-\frac{b+\sqrt{b^2-4ac}}{2c},$$

is stable at

$$\alpha\geqslant 2Bb/\sqrt{6}c,\ a\leqslant b^2/4c,$$

$$a\geqslant b^2/4c-\left(\sqrt{6}\,\frac{\alpha}{4B}\,\sqrt{c}-\frac{b}{2\sqrt{c}}\right)^2.$$

(3) The cubic ferromagnetic phase,

$$e_2=e_3=0,\ m_1=m_2=m_3=m/\sqrt{3},\ m^2=-\frac{\alpha}{\delta-4q/3},$$

is stable at $\alpha\leqslant 0$, $a\geqslant B^2/q$, where $q=|K|$.

(4) The tetragonal angular ferromagnetic phase,

$$m_1^2=m_2^2=-\frac{1}{3}\frac{\alpha}{\delta-4q/3}+\frac{Be_3}{\sqrt{6}q},$$

$$m_3^2=-\frac{1}{3}\frac{\alpha}{\delta-4q/3}-\frac{2Be_3}{\sqrt{6}q},$$

$$e_2=0,\ e_3=-\frac{b+\sqrt{b^2-4c(a-B^2/q)}}{2c},$$

is stable at

$$\alpha\leqslant-\sqrt{6}bB(\delta-4q/3)/4cq,\ a\leqslant b^2/4c+B^2/q,$$

$$a\geqslant\frac{b^2}{4c}+\frac{B^2}{q}-\left(\sqrt{\frac{2}{3}}\frac{q}{B}\,\frac{\alpha}{\delta-4q/3}\,\sqrt{c}+\frac{b}{2\sqrt{c}}\right)^2.$$

(5) The tetragonal collinear ferromagnetic phase,

$$m_1=m_2=0,\ m_3^2=-\frac{(\alpha+4Be_3/\sqrt{6})}{\delta},$$

$$e_2=0,\ ae_3+be_3^2+ce_3^3+\sqrt{\frac{2}{3}}Bm^2=0,$$

is stable at

$$\alpha\leqslant 0,\ a\leqslant\frac{b^2}{4c}+\frac{B^2}{q}-\left(\sqrt{\frac{2}{3}}\frac{q}{B}\,\frac{\alpha}{\delta-4q/3}\,\sqrt{c}+\frac{b}{2\sqrt{c}}\right)^2$$

and at

$$\alpha\geqslant 0,\ a\leqslant\frac{b^2}{4c}-\left(\sqrt{6}\,\frac{\alpha}{4B}\,\sqrt{c}-\frac{b}{2\sqrt{c}}\right)^2.$$

In the above formulas we assumed $K<0$. Thus, in the cubic ferromagnetic phase (3) the magnetization **M** is oriented along the crystallographic axis [111]. In the tetragonal angular ferromagnetic phase (4) the magnetization direction varies from axis [111] to [001] with temperature change. In the tetragonal collinear ferromagnetic phase (5), magnetization **M** is oriented along the crystallographic axis [001]. Because the crystallographic axes [001], [010], and [100] are equivalent, equal amounts of differently oriented tetragonal phase domains emerge. For the same reason, differently ori-

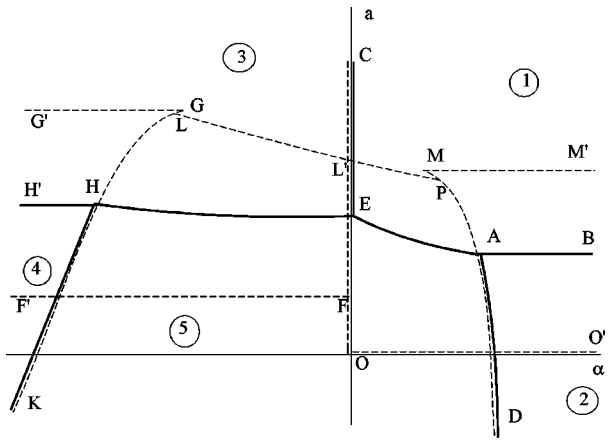

FIG. 6. Schematic phase diagram of a cubic ferromagnet on the α-a coordinates. The numbers denote different phases. The solid lines are lines of the phase transitions. The dotted lines represent the lines of the loss of equilibrium.

ented angular phase domains emerge in phase (4). In these phases the elastic deformations are equal to

$$e_2^2=3e_3^2;\quad e_3=-\frac{b+\sqrt{b^2-4c(a-B^2/q)}}{2c}. \tag{3}$$

Because phases (4) and (5) are both tetragonal, the phase transitions between them are isostructural.

The phase diagram of a ferromagnet on α-a coordinates is schematically shown in Fig. 6. The lines of phase transitions were determined from the conditions of the phases equilibria. From the paramagnetic cubic phase (1) the following phase transitions are possible. The AB line represents the first-order structural transition to the tetragonal paramagnetic phase (2). The CE line represents the second-order isostructural phase transition to the cubic ferromagnetic phase (3) with $\mathbf{M}\|[111]$. The line EA represents the combined magnetic and structural first-order phase transition to the tetragonal ferromagnetic phase (5). The second-order isostructural phase transition occurs on the AD line from the tetragonal paramagnetic phase (2) to the tetragonal ferromagnetic phase (5). The first-order combined structural and magnetic reorientational phase transitions occur on line HH' from the cubic ferromagnetic phase (3) to the tetragonal phase (4) and on line HE to the tetragonal phase (5). At last, the second-order isostructural magnetic reorientation phase transition occurs on line HK from the tetragonal phase (4) to the tetragonal phase (5). The loss-of-equilibrium lines are shown in Fig. 6 by dotted curves: for phase (1) it is CO and OO' lines, for phase (2) it is MM' and MD lines, for phase (3) it is CF and FF' lines, for phase (4) it is GG' and GK lines, for phase (5) it is KL, LP, and PD lines. The specific points of this phase diagram have the following coordinates: $A(8bB/3\sqrt{6}c, 2b^2/9c)$, $E(0, 2b^2/9c+4B^2/3\delta)$, $H(-2bB(\delta-4q/3)/\sqrt{6}cq, 2b^2/9c+B^2/q)$, $G(-\sqrt{\frac{3}{8}}bB(\delta-4q/3)/cq, b^2/4c+B^2/q)$, $L'(0, b^2/4c+4B^2/3\delta)$, $M(2bB/\sqrt{6}c, b^2/4c)$, $F(0, B^2/q)$.

In order to compare the results of calculations with experimental data, the α-a phase diagram can be represented on T-X coordinates. For this purpose we assume simple linear dependencies:

$$T_M=T_{M0}-2b^2/(9ca_0)-B^2/(qa_0)+\kappa X,\quad T_C=T_{C0}-\gamma X, \tag{4}$$

where T_{M0} and T_{C0} are the temperatures of martensitic and ferromagnetic phase transitions for the stoichiometric composition ($X=0$).

The lines of the main phase transitions on T-X coordinates are

$$(1)\Leftrightarrow(2):\quad T=T_{M0}-B^2/(qa_0)+\kappa X; \tag{5}$$

$$(1)\Leftrightarrow(3):\quad T=T_{C0}-\gamma X; \tag{6}$$

$$(3)\Leftrightarrow(4):\quad T=T_{M0}-\kappa X. \tag{7}$$

The phase diagram on T-X coordinates is shown in Fig. 7. The characteristic points of T-X phase diagram are

$$A{:}X_A=[T_{C0}-T_{M0}+8bB/(3\sqrt{6}c\alpha_0)+B^2/(qa_0)]/(\kappa+\gamma),$$

$$T_A=\{\kappa[T_{C0}+8bB/(3\sqrt{6}c\alpha_0)]+\gamma[T_{M0}-B^2/(qa_0)]\}/(\kappa+\gamma);$$

$$E{:}X_E=[T_{C0}-T_{M0}+B^2/(qa_0)-4B^2/(3\delta a_0)]/(\kappa+\gamma),$$

$$T_E=\{\kappa T_{C0}+\gamma[T_{M0}-B^2/(qa_0)+4B^2/(3\delta a_0)]\}/(\kappa+\gamma);$$

$$H{:}X_H=[T_{C0}-T_{M0}-2bB(\delta-4q/3)/(\sqrt{6}cq\alpha_0)]/(\kappa+\gamma),$$

$$T_H=\{\kappa[T_{C0}-2bB(\delta-4q/3)/(\sqrt{6}cq\alpha_0)]+\gamma T_{M0}\}/(\kappa+\gamma).$$

The best agreement of the theoretical T-X diagram with the experimental one (Fig. 5) is reached at the following values of the parameters: $T_{C0}\approx 375$ K, $T_{M0}\approx 200$ K, $\alpha_0=\delta/T_{C0}$, $a_0=b/T_{M0}$, $b/c\sim 0.1$, $b\sim 10^{11}$ J/m^3, $\delta/q\sim 10$, $\delta\sim 10^6$ J/m^3, $B\sim 10^6$ J/m^3, $\gamma\approx 295$ K, $\kappa\approx 800$ K.

B. The influence of a magnetic field

The influence of a magnetic field on the temperature of a first-order structural transition can be estimated using the thermodynamic Clapeiron-Clausius approach.[21]

At the phase equilibrium thermodynamic potentials Φ_M and Φ_A of martensitic and austenitic phases, as the functions of temperature T, magnetic field H, and pressure P, are equal

$$\Phi_M(T,H,P)=\Phi_A(T,H,P). \tag{8}$$

This equation defines the surface of phase transitions in the variables T,H,P. At the fixed point T_M, P_0, $H_0=0$ this surface is given by the equation

$$(\partial\Phi_M/\partial T-\partial\Phi_A/\partial T)\Delta T+(\partial\Phi_M/\partial H-\partial\Phi_A/\partial H)\Delta H+(\partial\Phi_M/\partial P-\partial\Phi_A/\partial P)\Delta P=0, \tag{9}$$

where $\Delta T=T-T_M$, $\Delta P=P-P_0$,

$$\partial\Phi_M/\partial T-\partial\Phi_A/\partial T=S_A-S_M=Q/T_M, \tag{10}$$

$$\partial\Phi_M/\partial H-\partial\Phi_A/\partial H=M_AV_A-M_MV_M, \tag{11}$$

$$\partial\Phi_M/\partial P-\partial\Phi_A/\partial P=V_M-V_A, \tag{12}$$

where S is entropy, Q is the hidden heat of martensitic phase transition at T_M, $M_{A,M}$ and $V_{A,M}$ are the magnetizations and the volumes of austenite and martensite, correspondingly.

Combining Eqs. (10)–(12) with Eq. (9), one can determine the magnetically driven shift of T_M at a constant pressure,

$$\Delta T=(M_MV_M-M_AV_A)HT_M/Q, \tag{13}$$

and the pressure-induced shift of T_M under a constant magnetic field,

$$\Delta T=(T_M/Q)(V_A-V_M)\Delta P. \tag{14}$$

Equation (13) describes the change of T_M in the case of both austenite and martensite being ferromagnetic.

In the case when $T_M>T_C$ both austenite and martensite at structural transformation are paramagnetic. Thus, the variation of T_M is

$$\Delta T=(\chi_MV_M-\chi_AV_A)H^2T_M/2Q, \tag{15}$$

where χ is the magnetic susceptibility.

Evidently, the most pronounced effect of the magnetic field on T_M can be achieved during the transition from paramagnetic austenite to ferromagnetic martensite:

$$\Delta T=M_MV_MHT_M/Q. \tag{16}$$

The shifts of T_M when subject to a magnetic field or pressure can be thus compared:

$$\Delta P=V_MM_MH/(V_A-V_M). \tag{17}$$

The latter expression is valid for the case of transition between ferromagnetic martensite and paramagnetic austenite.

V. DISCUSSION

In general, the results of these experimental studies correspond to each other and establish the general tendency of martensitic transition temperature T_M to increase and Curie temperature T_C to decrease with Ni excess in Ni_2MnGa. The composition dependencies of T_M and T_C obtained from the measurements of specific heat, magnetic susceptibility, and resistivity are shown in Fig. 5. It appears that the characteristic temperatures in $Ni_{2+x}Mn_{1-x}Ga$ merge at $x=0.18-0.20$. In the samples of this composition range the profiles of the observed singularities of every physical property changed qualitatively.

It can be seen that the experimentally obtained T-X phase diagram (Fig. 5) is in a qualitative agreement with the calculated one (Fig. 7). The detailed comparison of theory with experiment can be made on the basis of low-field magnetic susceptibility measurements. It can be seen that different sequences of phase transitions can be realized in $Ni_{2+x}Mn_{1-x}Ga$ of different compositions. According to Figs. 4 and 5 the temperature of magnetic phase transition from the cubic paramagnetic phase (1) to the cubic ferromagnetic phase (3) linearly decreases with concentration x. The temperature of the phase transition from the cubic ferromagnetic phase (3) to the tetragonal ferromagnetic phases (4) and

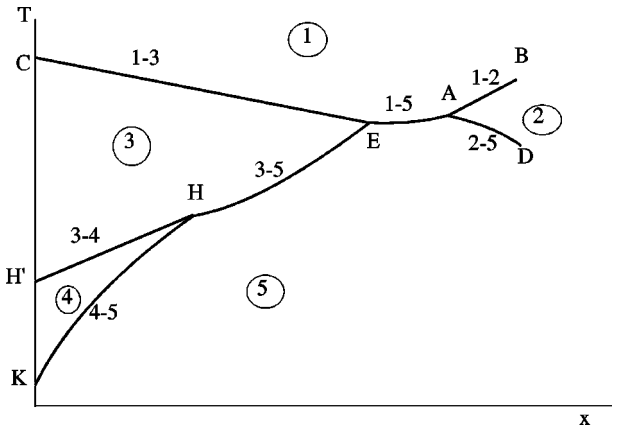

FIG. 7. Phase diagram of a cubic ferromagnet on the T-X coordinates.

(5) increases with concentration x. The appearance of an additional anomaly of low-field magnetic susceptibility at $T\approx260$ K for stoichiometric composition (Fig. 4) can be ascribed to the transition from the cubic ferromagnetic phase (3) to the tetragonal angular phase (4) (see Figs. 4 and 7). It is possible that this transition corresponds to premartensitic transition accompanied by the softening of the TA_2 phonon mode with wave vector $[1/3,1/3,0]$ (Refs. 5–12). The sharp drop of χ at $T\approx202$ K is due to orientational transition from phase (4) to phase (5).

The phase diagram of a ferromagnet was analyzed above in the absence of external stress and a magnetic field. Also, the domain structure of the samples was not taken into account. Appearance of structural and magnetic domains can result in the formation of domain phases with nonuniform distribution of magnetization. The first-order structural phase transition presupposes the coexistence of high-temperature austenite and low-temperature martensite. This coexistence occurs in a specific temperature range due to elastic strains that accompany the nucleation of the martensitic phase. The coherent and partially coherent conjugation of the phases on austenite-martensite boundaries results in the quasiperiodic structure of the martensitic domains. The formation of the martensitic domains is necessitated by the need to decrease the energy of elastic strains on the boundaries. The tetragonal distortions of the cubic lattice occur with the same probability along each of the crystallographically equivalent axes [001]. Hence, statistically equal amounts of differently oriented macrodomains appear in the sample. If the magnetic properties of the martensite and the austenite differ, the magnetic energy of each macrodomain will depend on its orientation with respect to an external magnetic field. The magnetic energy of a martensitic plate oriented along the magnetic field will be lower than that of a normally oriented martensitic plate.

In a low magnetic field at $T<T_M$ the lowering of the energy of demagnetization occurs via the formation of magnetic domains. When T_M and T_C are close to each other it is energetically favorable to create the intermediate state consisting of alternating ferromagnetic martensite and paramagnetic austenite domains. It is possible even in the absence of elastic strains on phase boundaries. At martensite-austenite phases coexistence, the additional increase of magnetization

occurs due to the magnetically induced transition of the residual austenite into martensite.

The experimental data obtained allow an estimate of some important physical parameters of the investigated alloys. Because the magnetization saturates at $H=160$ kA/m when $T>T_M$, the same value determines the field of magnetocrystalline anisotropy in the cubic phase. Let us estimate the field of magnetic anisotropy resulting from spontaneous deformations in the martensitic phase. The magnetoelastic part of the thermodynamic potential (1) is $\Phi_{ME}=G\lambda\Delta e\approx 10^4$ J/m^3, where G is the shift modulus of about 10^{11} J/m^3, $\lambda\sim 10^{-5}$ is the magnetostriction, Δe is the elastic deformation of about 10^{-2}. The estimated field of magnetic anisotropy appears to be $\Delta H_A=\Phi_{ME}/M_S\approx 8$ kA/m.

The magnetization of the tetragonal phase saturates at $H>800$ kA/m. This is comparable to the demagnetizing field $4\pi M$ of the martensitic domains. This indicates that the magnetization of crystal occurs through the reorientation of magnetic moments in unfavorably oriented macrodomains. Thus, the large value of the field of saturation in tetragonal martensite cannot be explained by the increase of a magnetocrystalline anisotropy only. The effective field of anisotropy $\Delta H_A\approx 8$ kA/m appears to be much lower than the demagnetizing field.

Using the data obtained it is possible to estimate the shift of martensitic transition temperature in a saturating magnetic field. Assuming the magnetization of saturation to be $M_S\sim 80$ kA/m at $H=800$ kA/m, the temperature of martensitic transformation $T_M\sim 300$ K, the hidden heat of transition $Q\sim 4\times 10^7$ J/m^3 we obtain $\Delta T\sim 5$ K in accordance with Eq. (13). Assuming that the relative change of the volume at martensitic transformation is $(V_M-V_A)/V_M\sim 10^{-2}$, let us estimate the pressure that results in the same change of transition temperature as the saturating magnetic field. Using expression (17) we obtain $\Delta P\sim 10^8$ Pa. This estimate is in qualitative agreement with experimental results of (Ref. 2): $dT_M/dP=-1.5$ K/kbar.

In conclusion, it was shown that the tetragonal phase of $Ni_{2+x}Mn_{1-x}Ga$ can be suppressed by Ni excess. The increase of Mn-Mn distances accompanying Ni excess reduces the Curie temperature of these alloys. The temperatures of martensitic and magnetic transitions merge at Ni excess $x=0.18-0.20$. Determining the correct composition of a magnetically driven shape-memory alloy is only the first step in realizing the effect described above. Further investigations are required to overcome the brittleness of this compound and to establish the relationship between martensitic and magnetic domain structures.

ACKNOWLEDGMENT

This work formed part of the Russian Foundation for Basic Research Grant-in-Aid No. 96-02-19755.

[1] P. J. Webster, K. R. A. Ziebeck, S. L. Town, and M. S. Peak, Philos. Mag. B **49**, 295 (1984).
[2] T. Kanomata, K. Shirakawa, and T. Kaneko, J. Magn. Magn. Mater. **65**, 76 (1987).
[3] V. V. Martynov and V. V. Kokorin, J. Phys. III **2**, 739 (1992).
[4] V. V. Kokorin, V. V. Martynov, and V. A. Chernenko, Scr. Metall. Mater. **26**, 175 (1992).
[5] G. Fritsch, V. V. Kokorin, and A. Kempf, J. Phys.: Condens. Matter **6**, L107 (1994).
[6] V. V. Kokorin, V. A. Chernenko, J. Pons, C. Segu, and E. Cesari, Solid State Commun. **101**, 7 (1997).
[7] L. Manosa, A. Gonzalez-Comas, E. Obrado, A. Planes, V. A. Chernenko, V. V. Kokorin, and E. Cesari, Phys. Rev. B **55**, 11 068 (1997).
[8] A. Zheludev, S. M. Shapiro, P. Wochner, A. Schwartz, M. Wall, and L. E. Tanner, Phys. Rev. B **51**, 11 310 (1995).
[9] A. Zheludev and S. M. Shapiro, Solid State Commun. **98**, 35 (1996).
[10] U. Stuhr, P. Vorderwisch, V. V. Kokorin, and P.-A. Lindgard, Phys. Rev. B **56**, 14 360 (1997).
[11] J. Worgull, E. Petti, and J. Trivisonno, Phys. Rev. B **54**, 15 695 (1996).
[12] T. E. Stenger and J. Trivisonno, Phys. Rev. B **57**, 2735 (1998).
[13] V. A. Chernenko, C. Segui, E. Cesari, J. Pons, and V. V. Kokorin, Phys. Rev. B **57**, 2659 (1998).
[14] V. V. Kokorin, V. A. Chernenko, V. I. Valkov, S. M. Konoplyuk, and E. A. Khapalyuk, Fiz. Tverd. Tela **37**, 3718 (1995) [Sov. Phys. Solid State **37**, 2049 (1995)].
[15] A. N. Vasil'ev, S. A. Klestov, R. Z. Levitin, V. V. Snegirev, V. V. Kokorin, and V. A. Chernenko, Zh. Eksp. Teor. Fiz. **109**, 973 (1996) [Sov. Phys. JETP **82**, 524 (1996)].
[16] K. Ullakko, J. K. Huang, C. Kantner, R. C. O'Handley, and V. V. Kokorin, Appl. Phys. Lett. **69**, 1966 (1996).
[17] S. Wirth, A. Leithe-Jasper, J. M. D. Coey, and A. N. Vasil'ev, J. Magn. Magn. Mater. **167**, L7 (1997).
[18] W. Hume-Rothery, J. Inst. Met. **35**, 295 (1926).
[19] J. Smit, J. Phys. F **8**, 2139 (1978).
[20] S. Fujii, S. Ishida, and S. Asano, J. Phys. Soc. Jpn. **58**, 3657 (1985).
[21] M. A. Krivoglaz and V. D. Sadovskii, Fiz. Met. Metalloved. **18**, 502 (1964) [Phys. Met. Metallogr. (USSR) **18**, No. 4 (1965)].